Research Article

Cancer Prevention Research

Didymin Induces Apoptosis by Inhibiting N-Myc and Upregulating RKIP in Neuroblastoma

Jyotsana Singhal[1], Lokesh Dalasanur Nagaprashantha[1], Rit Vatsyayan[2], Ashutosh[2], Sanjay Awasthi[1], and Sharad S. Singhal[1]

Abstract

Neuroblastomas arise from the neural crest cells and represent the most common solid tumors outside the nervous system in children. The amplification of N-Myc plays a primary role in the pathogenesis of neuroblastomas, whereas acquired mutations of *p53* lead to refractory and relapsed cases of neuroblastomas. In this regard, dietary compounds which can target N-Myc and exert anticancer effects independent of p53 status acquire significance in the management of neuroblastomas. Hence, we investigated the anticancer properties of the flavonoid didymin in neuroblastomas. Didymin effectively inhibited proliferation and induced apoptosis irrespective of p53 status in neuroblastomas. Didymin downregulated phosphoinositide 3-kinase, pAkt, Akt, vimentin, and upregulated RKIP levels. Didymin induced G_2/M arrest along with decreasing the levels of cyclin D1, CDK4, and cyclin B1. Importantly, didymin inhibited N-Myc as confirmed at protein, mRNA, and transcriptional level by promoter–reporter assays. High-performance liquid chromatography analysis of didymin-treated (2 mg/kg b.w.) mice serum revealed effective oral absorption with free didymin concentration of 2.1 μmol/L. Further *in vivo* mice xenograft studies revealed that didymin-treated (2 mg/kg b.w.) animals had significant reductions in tumors size compared with controls. Didymin strongly inhibited the proliferation (Ki67) and angiogenesis (CD31) markers, as well as N-Myc expression, as revealed by the histopathologic examination of paraffin-embedded section of resected tumors. Collectively, our *in vitro* and *in vivo* studies elucidated the anticancer properties and mechanisms of action of a novel, orally active, and palatable flavonoid didymin, which makes it a potential **n**ew **a**pproach for **n**euroblastoma **t**herapy (**NANT**) to target pediatric neuroblastomas. *Cancer Prev Res; 5(3); 473–83. ©2011 AACR.*

Introduction

Neuroblastomas are the neural crest–derived malignant tumors which constitute most common solid tumors in infants outside the central nervous system (1). More than 90% of the neuroblastomas are diagnosed before 5 years of age with greater occurrence of refractory and relapsed neuroblastomas in pediatric population over 18 months. Neuroblastomas metastasize to various sites such as skull, bones, spine, and retro-orbital tissues, which lead to challenging clinical presentations such as proptosis and retro-orbital ecchymosis in children (2–4). The major genetic causes for the incidence and therapeutic refractoriness of neuroblastomas include amplification of the oncogene N-Myc and loss of tumor suppressor p53 (5, 6). Raf-kinase inhibitory protein (RKIP) is a novel protein that interacts with MAP/ERK kinases and acts as an inhibitor of mitogen-activated protein kinase (MAPK) pathway (7). RKIP is an established metastasis suppressor protein and, given the role of MAPK pathway in regulating the survival and metastatic potential, RKIP has been the focus of recent investigations in assessing the effects of novel anticancer agents (8, 9). Loss of p53 leads to increased activity of multifunctional proteins, such as RLIP76, which mediate enhanced proliferation, invasion, and drug/radiation resistance in neuroblastoma (10, 11). In this regard, effective strategy for targeting the incidence of neuroblastoma in genetically identified risk groups should decrease the incidence of neuroblastoma, as well as improve the survival following initial diagnosis.

Given the limited 3-year event-free survival of 15% in the incident population and the nature of symptoms in affected children, validation of novel compounds becomes a vital focus of translational research to effectively target neuroblastomas. Also, due to the developing nervous and organ systems in children, the interventional choices will naturally favor active anticancer ingredients of safe dietary

Authors' Affiliations: [1]Department of Diabetes and Metabolic Disease Research, National Medical Center, Beckman Research Institute, City of Hope, Duarte, California; and [2]Department of Molecular Biology and Immunology, University of North Texas Health Science Center, Fort Worth, Texas

Corresponding Author: Sharad S. Singhal, Department of Diabetes and Metabolic Disease Research, National Medical Center, Beckman Research Institute, City of Hope, Duarte, CA 91010. Phone: 626-256-4673 (ext. 31238); Fax: 626-301-8136; E-mail: ssinghal@coh.org

doi: 10.1158/1940-6207.CAPR-11-0318

components, such as fruits, vegetables, and the compounds derived from them. Didymin is a flavonoid that is richly expressed in citrus fruits such as oranges, lemons as well as other dietary compounds such as mandarin and bergamot. Recently, it was reported that didymin can cause cell death in non–small cell lung cancer in a p53-independent manner (12). The use of chemotherapeutic drugs such as cisplatin, doxorubicin, and vincristine is highly limited in refractory and relapsed neuroblastomas due to frequent loss-of-function mutations in the tumor suppressor p53 (13, 14). Hence, the elucidation of signaling pathways through which didymin acts in neuroblastomas would have potential implications toward the effective management of neuroblastomas. In this regard, we investigated the efficacy and mechanisms of action of didymin *in vitro* cultures and *in vivo* mice xenograft models of neuroblastomas.

Our studies first focused on testing the effect of didymin on the survival and clonogenic potential of both p53 wild type and p53 mutant neuroblastomas. Next, we investigated the induction of apoptosis followed by analyzing the impact on key nodes of proliferation in neuroblastomas. Cell-cycle analysis revealed a mechanism of action of didymin that includes its ability to regulate cyclin signaling downstream of p53. Importantly, we investigated the effect of didymin on N-Myc by Western blot, mRNA, and N-Myc luciferase promoter–reporter assays followed by *in vivo* mice xenograft studies. Our studies revealed the ability of didymin to regulate important nodes of signaling along with being effective, irrespective of p53 status in neuroblastomas.

Materials and Methods

Reagents

Didymin, hesperidin, and 2′-hydroxyflavanone (2HF; purity >98%) were purchased from Indofine Chemical Company. PARP, cyclin B1, cyclin D1, CDK4, Akt, pAkt (S^{473}), glyceraldehyde-3-phosphate dehydrogenase (GAPDH), N-Myc, Ki67, CD31, and RKIP antibodies were purchased from Santa Cruz Biotechnology, Upstate Cell Signaling, and Cell Signaling Technologies. The siGENOME smart pool siRNA for RKIP and control scrambled siRNA were purchased from Dharmacon. APO LOGIX carboxyfluorescein (FAM) Caspase Detection Kit was purchased from Cell Technology. Lipofectamine 2000 and fluorescein isothiocyanate (FITC)-labeled Annexin V Conjugate Detection Kit were purchased from Invitrogen. The thymidine kinase promoter–driven *Renilla* luciferase (pTK-RL) and terminal deoxynucleotidyl-transferase dUTP nick-end labeling (TUNEL) Fluorescence Kit were obtained from Promega. Avidin/biotin complex (ABC) Detection Kit was purchased from Vector.

Cell lines and cultures

CHLA-90 and SK-N-BE2 (p53 mutant) as well as SMS-KCNR and LAN-5 (p53 wild-type) human neuroblastoma cell lines were kindly authenticated and provided in May 2010 by Dr. Patrick Reynolds, Children's Neuroblastoma Cancer Foundation/Children Oncology group, Texas Tech University, School of Medicine, Lubbock, TX. The authentication of cell lines was done by analyzing 15 different human short-tandem repeat (STR; carried out by Center for Investigative Genetics core facility at University of North Texas Health Science Center, Fort Worth, TX) to test for interspecies contamination. The cell lines were last tested in April 2011. Cells were grown in complete medium consisting of Iscove's modified Dulbecco's medium supplemented with 3 mmol/L L-glutamine, 5 μg/mL each of insulin and transferrin, 5 ng/mL of selenous acid (ITS culture supplement), and 20% FBS at 37°C in a humidified 5% CO_2 atmosphere. Cell lines were subcultured by detaching without trypsin from culture plates by using a modified Puck's Solution A plus EDTA (Puck's EDTA), which contain 140 mmol/L NaCl, 5 mmol/L KCl, 5.5 mmol/L glucose, 4 mmol/L NaHCO3, 0.8 mmol/L EDTA, 13 mmol/L phenol red, and 9 mmol/L HEPES buffer (pH 7.3). All the cells were also tested for *Mycoplasma* once every 3 months.

Drug sensitivity (MTT) assay

Cell density measurements were done by a hemacytometer to count dye-excluding cells resistant to staining with trypan blue. Approximately 2×10^4 cells were plated into each well of a 96-well flat-bottomed microtiter plate 24 hours prior to addition of medium containing varying concentrations of indicated flavonoids. After 12 hours of incubation, indicated flavonoids (didymin, hesperidin, 2HF; ranging from 0–200 μmol/L each) were added to 8 replicate wells. After 48 hours of incubation, 20 μL (5 mg/mL stock) MTT was added to each well and incubated for 2 hours at 37°C. The plates were centrifuged and medium was removed. Formazan dye trapped in cells was dissolved by addition of 100 μL dimethyl sulfoxide with gentle shaking for 2 hours at room temperature, followed by measurement of absorbance at 570 nm (15–17).

siRNA mediated knockdown of RKIP

The desalted RKIP siRNA (Dharmacon) was resuspended in 1× universal buffer provided by Dharmacon Research laboratory. Cells were transfected with scrambled and RKIP siRNA at the concentration of 1 μg/mL in serum-free medium, using Lipofectamine 2000 (Invitrogen) for 3 hours, according to the manufacturer's instructions. Excess siRNA was washed off with PBS and complete medium (i.e., with FBS) was added. After 24-hour silencing, cells were exposed with 50 μmol/L didymin. After 48-hour incubation, MTT assays as well as Western blot analyses for RKIP and N-Myc expression were done as described previously (18–20).

Colony-forming assay

Cell survival was evaluated using a standard colony-forming assay. A total of 1×10^5 cells/mL were incubated with 1 of the 3 drugs (didymin, hesperidin, 2HF-50 μmol/L each) for 48 hours, and aliquots of 50 or 100 μL were added to 60-mm size Petri dishes containing 4 mL culture medium. After 10 days, adherent colonies were fixed, stained with 0.5% methylene blue for 30 minutes, and counted using the Innotech Alpha Imager HP (21).

In situ caspase-3 cleavage assay

Detection of active caspase-3 in live cell cultures was carried out using an APO LOGIX carboxyfluorescein (FAM) Caspase Detection Kit (Cell Technology). The kit detects active caspase-3 in living cells through FAM-labeled DEVD fluoromethyl ketone (FMK), which irreversibly binds to active caspase-3. The inhibitor is cell permeable and noncytotoxic. The assay was carried out according to manufacturer's instructions (22).

Terminal deoxynucleotidyl-transferase dUTP nick-end labeling assay

For measurement of apoptosis by TUNEL assay, 1×10^5 cells were grown on the cover slips for approximately 12 hours followed by treatment with test compounds (didymin, hesperidin, and 2HF 50 μmol/L each) for 24 hours. Apoptosis was determined by the labeling of DNA fragments with TUNEL using Promega fluorescence apoptosis detection system. Slides were analyzed under a fluorescence microscope using a standard fluorescein filter set to view the green fluorescence at 520 nm and red fluorescence of propidium iodide at more than 620 nm (17).

In vitro migration assay

Cell migration was determined using a wound healing assay (23). A total of 2×10^4 CHLA-90 and SMS-KCNR cells were seeded in 6-well plates to reach 100% confluence within 24 hours and then treated with 10 μmol/L mitomycin C for 2 hours. Subsequently, a similarly sized scratch was made with a 200-μL pipette tip across the center of each well and immediately imaged at baseline and then at 24 hours in control- and didymin-treated groups by using an Olympus Provis AX70 microscope. The rate of cell migration was determined by comparing the sizes of scratch area using ImageJ software.

Western blot analysis

The control and 50 μmol/L didymin-treated (at 24 hours) cells were lysed and analyzed by Western blot analyses for PARP cleavage, phosphoinositide 3-kinase (PI3K; $Y^{458/199}$), pAkt (S^{473}), AKT, cyclin D1, cyclin B1, CDK4, N-Myc, RKIP, and vimentin by using specific antibodies. Briefly, lysates containing approximately 50 μg of proteins were subjected to SDS-PAGE and proteins were transferred onto nitrocellulose membrane. After blocking with 5% non-fat dry milk, the membrane was incubated overnight with the desired primary antibody (1:1,000 dilution). Subsequently, the membrane was incubated with appropriate secondary antibody for 2 hours, and the immune-reactive bands were visualized using the Enhanced Chemiluminescence Kit from Perkin-Elmer according to the manufacturer's instructions. The same membrane was reprobed with the antibody against GAPDH (1:5,000 dilution) as an internal control for equal protein loading. The intensity of immune-reactive bands on Western blots was determined using a densitometer (Molecular Dynamics) equipped with Image QuaNT software.

Flow cytometry analysis of cell-cycle regulation

A total of 2×10^5 cells were treated with didymin (50 μmol/L) for 18 hours at 37°C. After treatment, floating and adherent cells were collected, washed with PBS, and fixed with 70% ethanol. On the day of flow analysis, cell suspensions were centrifuged; counted, and same numbers of cells were resuspended in 500 μL PBS in flow cytometry tubes. Cells were then incubated with 2.5 μL of RNase (stock 20 mg/mL) at 37°C for 30 minutes after which they were treated with 10 μL of propidium iodide (stock 1 mg/mL) solution and then incubated at room temperature for 30 minutes in the dark. The stained cells were analyzed using the Beckman Coulter Cytomics FC500, Flow Cytometry Analyzer. Results were processed using CXP2.2 analysis software from Beckman Coulter (17).

RT-PCR analysis

Expression of N-Myc mRNA in neuroblastomas was evaluated by reverse transcriptase PCR (RT-PCR) analysis. The RNA from control and experimental groups was prepared 24 hours after didymin treatment using an Rneasy Kit (Qiagen) was quantified and 2 μg RNA was subjected to 1% agarose gel electrophoresis in MOPS-formaldehyde buffer. N-Myc gene-specific primers were used for RT-PCR (Biosynthesis Inc.; ref. 24). RT-PCR one step kit was used according to the manufacturer's instructions (Qiagen). Level of N-Myc protein in control- and didymin-treated cells were also measured by immunoassay using anti-NMyc IgG. Aliquots of crude cell extracts containing approximately 50 μg protein were applied to SDS-PAGE and Western blot analyses were done.

N-Myc promoter–reporter assay

CHLA-90 and SMS-KCNR cells were cultured as adherent monolayers in a 96-well plate at a density of 2×10^4 cells per well. The Firefly luciferase reporter construct (0.4 μg, pEB-Luc-N-Myc), kindly gifted by Prof. William L. Carroll, New York University Medical Center, NY, was cotransfected with 100 ng of *Renilla* luciferase construct (thymidine kinase promoter–driven *Renilla* luciferase; pTK-RL) by Lipofectamine Reagent according to the manufacturer's instructions (Invitrogen). After 24 hours of incubation, transfected cells were treated with 50 μmol/L of didymin. At 24-hour post-treatment, promoter activity was measured as luciferase activity by mixing cells with 50 μL of passive lysis buffer (Promega), followed by 15 minutes of shaking at room temperature. On a luminometer plate, 20 μL of the lysate was then mixed with 100 μL of luciferase assay reagent followed by 100 μL of Stop N′ Glo Buffer (Promega). Luciferase activity was then determined as a ratio of Firefly to *Renilla* luciferase. *Renilla* luciferase activity was thus used as an internal control.

High-performance liquid chromatography analysis of didymin in serum

Mice ($n = 3$ each for control and didymin treatment) were administered either 0.1 mL corn oil or 50 μg didymin/0.1 mL corn oil/mice (2 mg/kg b.w.) by oral gavage on alternate

days for 8 weeks. On the last day, the blood was collected within 1 hour after final dosage. The 100 μL of serum was subjected to protein precipitation using 200 μL of methanol. The sample was centrifuged at 13,300 rpm for 15 minutes at 4°C and the clear supernatant was lyophilized. The resulting pellet was dissolved in 200 μL of methanol: 0.2% phosphoric acid buffer (58:42 v/v). The 25 μL of each sample was subjected to high-performance liquid chromatography (HPLC) analysis using C_{18} reverse-phase column at wavelength of 295 nm on Agilent 1100 system with auto injector (Agilent Technologies). The mobile phase consisting of acetonitrile (ACN) and water at a flow rate of 1.0 mL/min with following gradient: 0–1 minute: ACN-10%, H_2O-90%; 1–2 minutes: gradually increasing to ACN-20%, H_2O-80%; 2–14 minutes: gradually changing to ACN-90%, H_2O-10%; 14–16 minutes: ACN-10%, H_2O-90%.

In vivo xenograft studies

Hsd: Athymic nude nu/nu mice were obtained from Harlan. All animal experiments were carried out in accordance with a protocol approved by the Institutional Animal Care and Use Committee (IACUC). The 11-week-old mice ($n = 10$) were divided into 2 groups of 5 animals [(For treatment with (i) corn oil (vehicle), (ii) didymin (2 mg/kg b.w.)]. The animals were injected with 2×10^6 SMS-KCNR neuroblastoma cell suspensions in 100 μL of PBS, subcutaneously into one flank of each nu/nu nude mouse. At the same time, animals were randomized into treatment groups as indicated in Figure 5. Treatment was started 10 days after the neuroblastoma cells implantation to see palpable tumor growth. Treatment consisted of didymin (2 mg/kg b.w.) in 100 μL corn oil by oral gavage alternate day. Control groups were treated with 100 μL corn oil by oral gavage alternate day. Animals were examined daily for signs of tumor growth. Tumors were measured in 2 dimensions using calipers. Photographs of animals were taken at days 1, 10, 20, 40, and 60 after subcutaneous injection, are shown for all groups. Photographs of tumors were also taken at day 60.

Histopathologic examination of tumors for angiogenic, proliferative, and differentiation markers

Tumors from SMS-KCNR neuroblastoma mice xenografts (control and didymin treated) were harvested on day 60. Tumor samples fixed in buffered formalin for 12 hours were processed conventionally for paraffin-embedded tumor sections (5-μm thick). Histopathologic analyses with ki67, anti-CD31, and N-Myc were carried out using Universal ABC Detection kit (Vector). The sections were examined under Olympus Provis AX70 microscope connected to a Nikon camera.

Statistical analyses

All data were evaluated with a 2-tailed unpaired Student *t* test and are expressed as mean ± SD. The statistical significance of differences between control and treatment groups was determined by ANOVA, followed by multiple comparison tests. Changes in tumor size and body weight during the course of the experiments were visualized by scatter plot. Differences were considered statistically significant when the *P* value was less than 0.05.

Results

Antiproliferative effect of didymin in neuroblastoma

The cell survival study by MTT assay revealed that didymin is the most potent of the 3 flavonoids tested in 4 neuroblastomas cell lines [CHLA-90 and SK-N-BE2 (p53-mutant) as well as SMS-KCNR and LAN-5 (p53 wild-type)]. The other flavonoid hesperidin was less effective and 2HF was not much effective against the 4 neuroblastoma cell lines tested. The 50 μmol/L didymin caused approximately 75% cell death, whereas hesperidin induced only approximately 35% cell death and 2HF induced approximately 10% cell death in all tested neuroblastoma cell lines at similar concentrations. Didymin did not cause any cytotoxicity in normal human umbilical vein endothelial cells (HUVEC) in MTT assay (Fig. 1A). The ability of didymin to arrest the growth of neuroblastoma tumors was further evident in colony-forming assay in which 50 μmol/L didymin caused approximately 70% growth inhibition, as compared with hesperidin (approximately 30% growth inhibition) and 2HF (approximately 10% growth inhibition; Fig. 1B). Thus, didymin decreased both survival and clonogenic potential to a greater extent than hesperidin and 2HF in neuroblastomas, as revealed by MTT and colony-forming assays, respectively. The effect of didymin on apoptosis was further studied by TUNEL apoptosis assay. The didymin treatment induced enhanced cell death relative to hesperidin and 2HF in neuroblastoma, which was evident by increased green fluorescence, a measure of DNA strand breaks induced by apoptosis in TUNEL apoptotic assay (Fig. 2A; ref. 25). Didymin also effectively inhibited the migration of neuroblastoma cells *in vitro* wound healing assay relative to hesperidin and 2HF (Fig. 2B). These findings collectively confirmed the enhanced cytotoxic potential of didymin in targeting neuroblastomas relative to hesperidin and 2HF. Following initial assessment of the potent anticancer properties of didymin in neuroblastomas, we next carried out detailed mechanistic studies in CHLA-90 (p53 mutant) and SMS-KCNR (p53 wild type) neuroblastoma cells.

Proapoptotic and antimigratory effect of didymin in neuroblastoma

The didymin treatment increased caspase-3 activation in *in situ* caspase-3 cleavage assay as revealed by enhanced green fluorescence in the treated group compared with controls (Fig. 2C). Western blot revealed the enhanced PARP cleavage consequent to didymin treatment in neuroblastomas. Didymin treatment also decreased the levels of PI3K, phosphorylation, and protein levels of Akt. Didymin also effectively reduced the levels of vimentin, a major intermediate filament protein which regulates epithelial–mesenchymal transition, an essential process during oncogenic transformation as well as metastasis (Fig. 2D). These

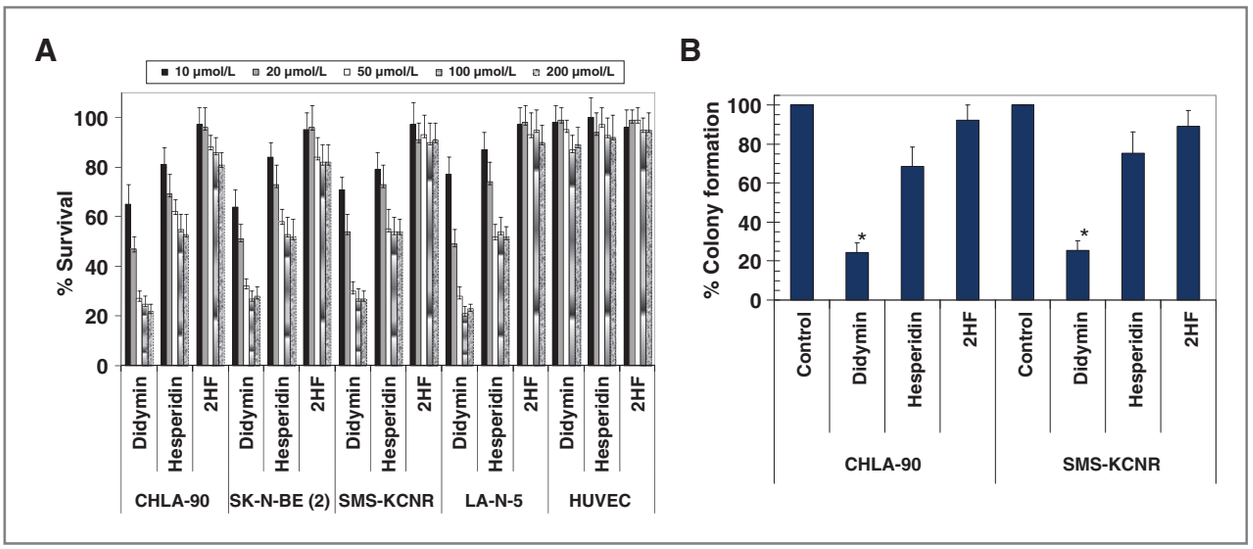

Figure 1. Antiproliferative effect of didymin in neuroblastoma. Drug sensitivity assays were carried out by MTT assay using didymin, hesperidin, and 2HF at 48-hour posttreatment to determine IC_{50}. Values are presented as mean ± SD from 2 separate determinations with 8 replicates each ($n = 16$; A). Colony-forming assay was carried out as described in Methods. The colonies were counted using Innotech Alpha Imager HP (21). *, $P < 0.001$ compared with control (B).

results provided the mechanistic rationale for the decreased survival and clonogenic potential induced by didymin, as revealed by our studies by revealing the inhibition of PI3K and pAkt by didymin. The activation of caspase-3 and enhanced PARP cleavage further validated the apoptosis observed by TUNEL apoptosis assay following didymin treatment. The expression of vimentin is associated with enhanced motility of tumor cells and hence inhibition of vimentin by didymin was significant in the context of antimigratory effects of didymin in neuroblastomas as revealed by *in vitro* migration assay (26, 27). Thus, these results provided further corroborative evidence for the observed antiproliferative and proapoptotic effects of didymin in initial cell survival, clonogenic, and apoptosis studies.

Effect of didymin on cell-cycle progression in neuroblastoma

We next analyzed the effect of didymin on cell-cycle progression by fluorescence-activated cell sorting (FACS) analysis. Loss of p53 leads to decreased cell-cycle checkpoint regulation which favors enhanced proliferation of cells (28–30). Didymin caused significant G_2/M phase arrest in CHLA-90 (p53 mutant) and SMS-KCNR (p53 wild type) neuroblastoma cells, suggesting the inhibition of cell cycle as an additional mechanism for the antiproliferative effects of didymin (Fig. 3A). Western blot of didymin-treated neuroblastoma cells revealed decrease in cyclin B1, cyclin D1, and CDK4 (Fig. 3B). Cyclin D1 is a key G_2/M phase regulator whose increase during G_2 phase leads to progression to mitosis and hence the decrease of cyclin D1 by didymin impacts G_2/M phase progression (31–33). Another interesting finding was that we observed a decrease in the levels of CDK4, the kinase which is commonly associated with G_1 transition along with G_2/M phase arrest. CDK4 has multiple functions and has been also investigated for its role in G_2/M transition. It has been shown that overexpression of dominant-negative CDK4 leads to arrest of G_2 phase progression (33). Some of the anticancer compounds such as apigenin and thimerosal also cause inhibition of CDK4 along with cyclin B1, while causing G_2/M phase arrest (33–35). Cyclin B1, the regulatory subunit of cdc2 kinase, is required for mitotic phase initiation. Cyclin B1 is localized to kinetochores during cell division and regulates the alignment of chromosomes during mitosis (36). The p53 activation leads to G_2/M phase arrest by decreasing the levels of cyclin B1 levels as well as inhibiting the activity of cyclin B1 promoter, whereas the activation of cyclin B1 leads to cell-cycle progression even in the presence of p53 activation (37, 38). Thus, cyclin B1 is a critical requirement and mediator of G_2/M phase progression downstream of p53. In this context, the ability of didymin to downregulate cyclin B1 in both p53 mutant and p53 wild type neuroblastomas represents a potentially significant mechanism of action for the observed antiproliferative effects of didymin in neuroblastomas, irrespective of p53 status.

Impact of didymin on N-Myc expression

The amplification of N-Myc contributes both to pathogenesis and aggressive progression of neuroblastomas, giving them a highly angiogenic phenotype (5, 39). Hence, we analyzed the impact of didymin on N-Myc expression. The didymin treatment decreased the levels of N-Myc protein in a time- and concentration-dependent manner as shown by Western blot analyses (Fig. 3C). The 50 μmol/L didymin treatment induced approximately 5-fold reduction in N-Myc mRNA levels as revealed by RT-PCR using N-Myc gene-specific primers (Fig. 3D). We further explored whether didymin regulates N-Myc promoter activity by luciferase

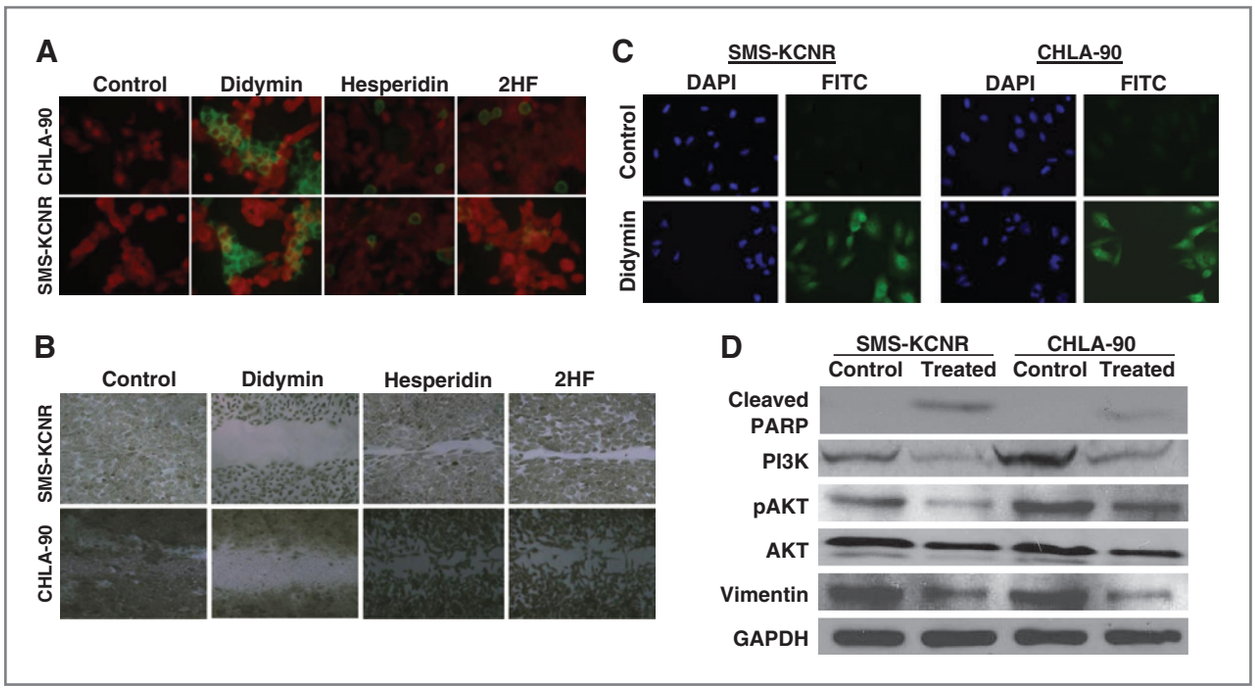

Figure 2. Proapoptotic and antimigratory effects of didymin in neuroblastoma. For TUNEL apoptosis assay, cells were grown on cover slips and treated with 50 μmol/L didymin for 24 hours. TUNEL assay was carried out using Promega Fluorescence Detection Kit and examined using Zeiss LSM 510 META laser scanning fluorescence microscope with filters 520 and more than 620 nm. Photographs taken at identical exposure at ×400 magnification are presented. Apoptotic cells showed green fluorescence (A). The *in vitro* migration assay shows that the didymin inhibits neuroblastoma cell migration in wound healing assay (B). For caspase activation detection, SMS-KCNR and CHLA-90 cells were plated on glass cover slip in tissue culture–treated 12-well plates and incubated with 50 μmol/L of didymin for 24 hours at 37°C. Apoptotic cells were detected by staining with 5 μmol/L caspase FITC–VAD–FMK (Promega) *in situ* marker for 30 minutes (C). Analysis of the effect of didymin on PARP cleavage, PI3K, and Akt activation by Western blot: The control and 50 μmol/L didymin-treated cells were lysed and analyzed by Western blot for PARP cleavage, PI3K ($Y^{458/199}$), pAkt (S^{473}), AKT, and vimentin by using specific antibodies. Membranes were stripped and reprobed for GAPDH as a loading control (D). DAPI, 4′,6-diamidino-2-phenylindole.

promoter–reporter assays. The Firefly luciferase reporter construct (0.4 μg pEB-Luc-N-Myc) was cotransfected with 100 ng of *Renilla* luciferase plasmid construct (thymidine kinase promoter–driven *Renilla* luciferase; pTK-RL) by Lipofectamine reagent. After 24 hours of incubation, the transfected cells were treated with 50 μmol/L of didymin, further incubated for 24 hours, and the luciferase assay was done. Didymin treatment induced significant decrease in the activity of N-Myc promoter compared with controls (Fig. 4A).

PI3K inhibition mediated downregulation of N-Myc protein levels has been reported (40). Didymin caused significant inhibition of PI3K in neuroblastomas (Fig. 2D). RKIP can inhibit MAPK and Myc signaling (41–43). Interestingly, RKIP overexpression is also known to positively induce normal neuronal differentiation in neuroblastoma (44). Hence, we examined the effect of didymin on RKIP expression. Didymin significantly enhanced the levels of RKIP in both p53 mutant (CHLA-90) and p53 wild type (SMS-KCNR) neuroblastomas (Fig. 4B). Given the significant role of RKIP in tumor signaling, we further studied the impact of knockdown of RKIP in SMS-KCNR and CHLA-90 neuroblastoma cells. The MTT assay following knockdown of RKIP by siRNA treatment revealed partial reversal of the didymin-induced inhibition of neuroblastoma cell survival (data not shown). The knockdown of RKIP was also associated with an increase in the expression of N-Myc in neuroblastoma cells. The knockdown of RKIP also caused a partial reversal in the didymin-induced decrease of N-Myc expression as detected by Western blot analyses (Fig. 4C). This observed inhibitory effect of RKIP on N-Myc expression is in accordance with previous studies implicating the role of RKIP in regulation of Myc expression (42). Hence, RKIP upregulation, along with N-Myc repression, represents a potent mechanism of action of didymin of specific relevance in inducing its anticancer effects in neuroblastomas. The collective antiproliferative, antimigratory, and proapoptotic effects of didymin *in vitro*, along with its ability to inhibit N-Myc, PI3K/Akt, and MAPK signaling pathways which play a significant mechanistic role in the incidence, progression, and clinical refractoriness of neuroblastomas, provided strong rationale for the further investigation of didymin in *in vivo* mice xenograft studies.

Antineoplastic effect of didymin *in vivo*

We first assessed the absorption of orally administered didymin in mice. HPLC analysis of didymin-treated mice serum revealed that didymin is effectively absorbed after

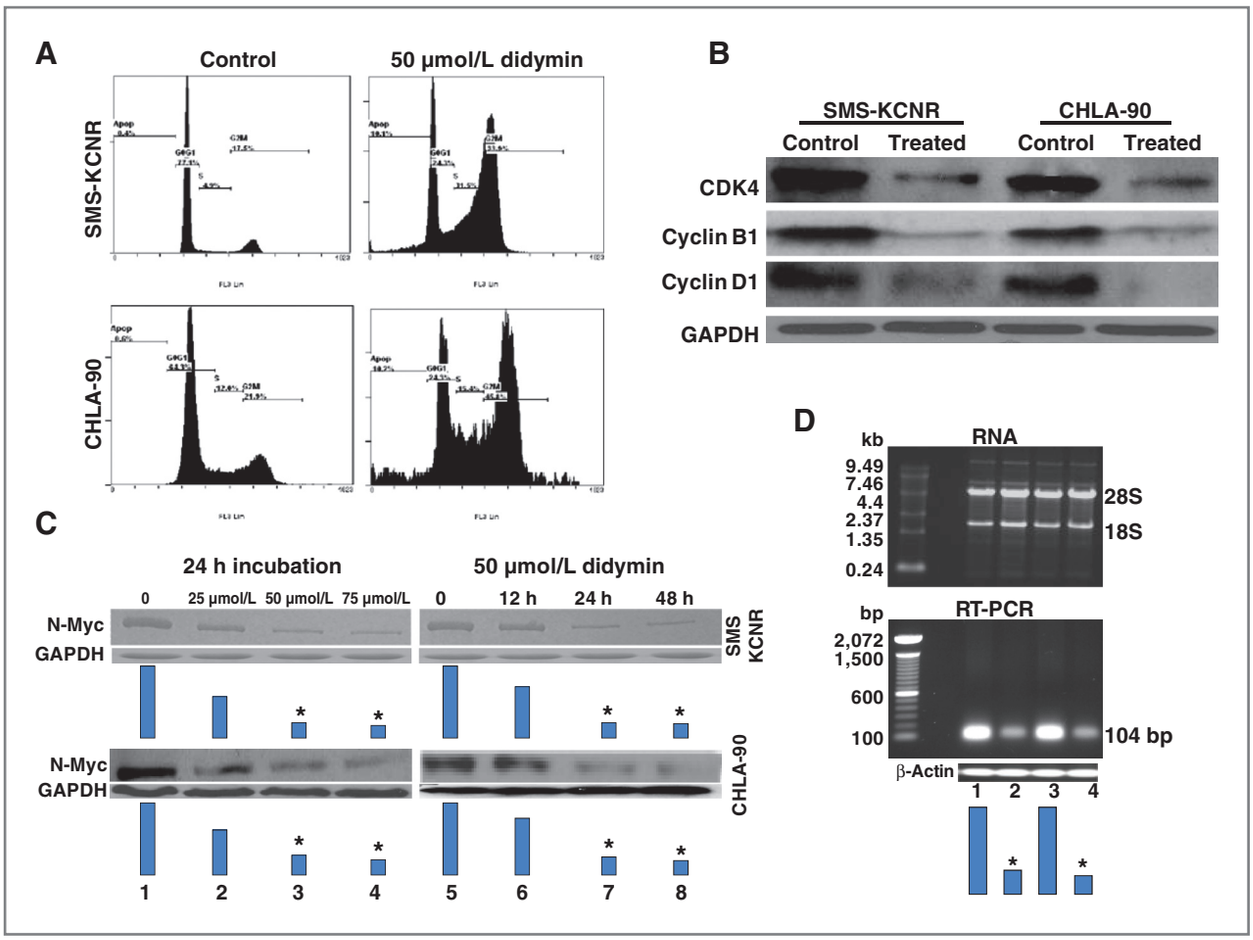

Figure 3. Effect of didymin on cell cycle and N-Myc levels in neuroblastoma. Inhibitory effect of didymin on cell-cycle distribution was determined by FACS analysis. Experimental details are given in the Methods section. The stained cells were analyzed using the Beckman Coulter Cytomics FC500, Flow Cytometry Analyzer. The experiment was repeated 3 times and similar results were obtained (A). The 50 μmol/L didymin-treated cells were processed for Western blot analyses for cyclin D1, cyclin B1, and CDK4 expression by using specific antibodies. Membranes were stripped and reprobed for GAPDH as a loading control (B). The SMS-KCNR and CHLA-90 cells were treated with didymin and the effect on N-Myc protein level using anti-N-Myc IgG was determined in a concentration- and time-dependent study. Results were quantified by scanning densitometry (C). The mRNA level of N-Myc following 50 μmol/L didymin treatment was assessed by RT-PCR using N-Myc gene-specific primers (Biosynthesis Inc.). Total RNA after 50 μmol/L didymin treatment (top, D) and N-Myc mRNA by RT-PCR (bottom D): Lane 1, SMS-KCNR, Lane 2, SMS-KCNR didymin treated, Lane 3, CHLA-90, Lane 4, CHLA-90 didymin treated. Bars represents densitometry and *, *P* value less than 0.001 compared with control.

oral dosage and it reaches a serum concentration of 2.1 μmol/L (Fig. 4D). It is important to note that we quantified only didymin, but not its metabolites, to address whether didymin, a relatively new flavonoid in cancer research, is absorbed following oral administration.

We next assessed the regression of neuroblastoma mice xenografts following oral administration of didymin. The mice harboring SMS-KCNR neuroblastoma xenografts were treated with 50 μg/mice (equivalent to 2 mg/kg b.w. or 0.0002% w/w) of didymin in 100 μL corn oil alternate day for 60 days by oral gavage. Control group was treated with 100 μL corn oil. Treatment was started 10 days post neuroblastoma cells implantation after a palpable tumor growth was observed. Photographs of animals were taken at days 1, 10, 20, and 40 after subcutaneous injection are shown for both groups. Tumors were dissected at day 60, photographed and weighed. Didymin-treated animals had significant reductions in tumors as compared with control, whereas uncontrolled growth was observed in the control groups. The didymin-treated mice were active and weight gain was comparable with nontumor–bearing controls, and no overt toxicity was evident (Fig. 5A). The final tumor weight on day 60 was 0.91 g in didymin-treated group compared with 1.97 g in controls. Present studies, for the first time, showed sustained regression of xenografts of neuroblastomas by didymin (Fig. 5B and C).

The effect of didymin treatment on the neuroblastoma progression markers in resected mice xenograft sections was further examined. The histopathologic examination of paraffin-embedded tumor xenograft sections revealed the

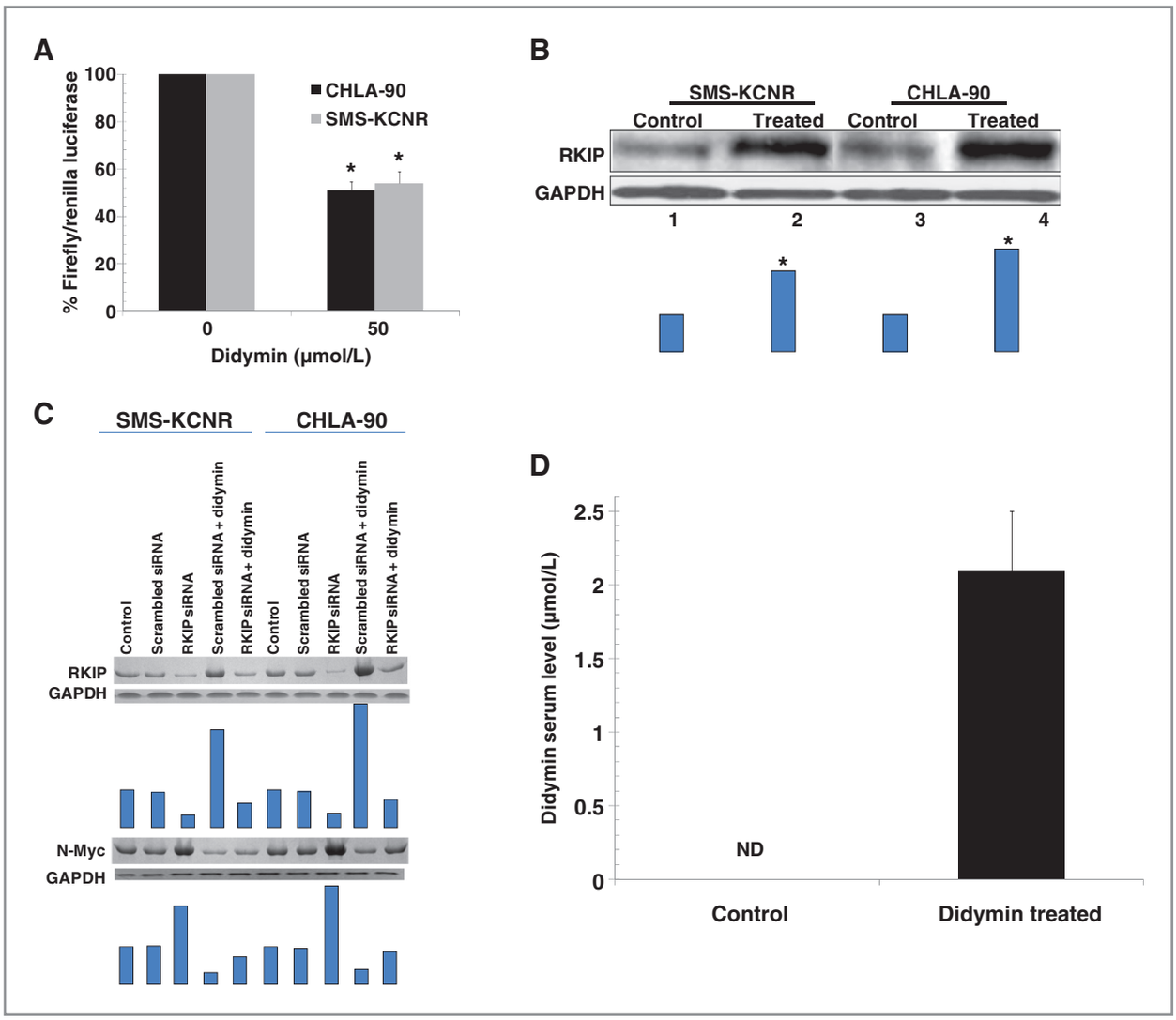

Figure 4. Effect of didymin on N-Myc promoter activity and RKIP expression. Downregulation of luciferase activity upon didymin treatment: Upon transfection with the N-Myc luciferase reporter construct or a control construct along with a *Renilla* luciferase vector and followed by 24-hour treatment with 50 μmol/L didymin, luciferase activities were measured. A significant decrease in the relative activity of the N-Myc luciferase reporter assay was observed in didymin-treated cells as compared with that of controls. *, $P < 0.001$ compared with control (A). Western blot for RKIP expression 24 hours after 50 μmol/L didymin treatment: Bars represents densitometry and *, P value less than 0.005 compared with control (B). After knockdown of RKIP by siRNA, the levels of RKIP and N-Myc were detected by Western blot analyses. Membranes were stripped and reprobed for GAPDH as a loading control. Results were quantified by scanning densitometry (C), and the concentration of didymin in mice serum by HPLC analysis: Didymin concentration was determined after 1 hour of final oral dosage (50 μg or 2 mg/kg b.w.) in mice serum. Bar represents the quantification (mean ± SD) of didymin in mice serum ($n = 3$). ND, not detectable (D).

decreased levels of proliferation marker, Ki67, angiogenesis marker, CD31, and N-Myc expression in SMS-KCNR neuroblastoma after didymin treatment, which further supported our *in vitro* results (Fig. 5D).

Discussion

Until today, there are no safe dietary choices to prevent the incidence and progression of neuroblastomas in children. The use of chemotherapeutic drugs, radiation, and surgical approaches are often coupled with recurrent and diverse clinical challenges such as limitations of young age, as well as amplification of off-target cytotoxicity on developing nervous and skeletal systems, over the course of time following initial therapy in children. In this regard, our current studies, for the first time, have revealed that the novel flavonoid didymin is effective against neuroblastomas both *in vitro* cell cultures and *in vivo* mice xenograft studies. Didymin effectively inhibited the proliferation of neuroblastomas and induced apoptosis by inhibiting PI3K, Akt, and increasing RKIP levels. Didymin also decreased the levels of vimentin, a marker of epithelial–mesenchymal

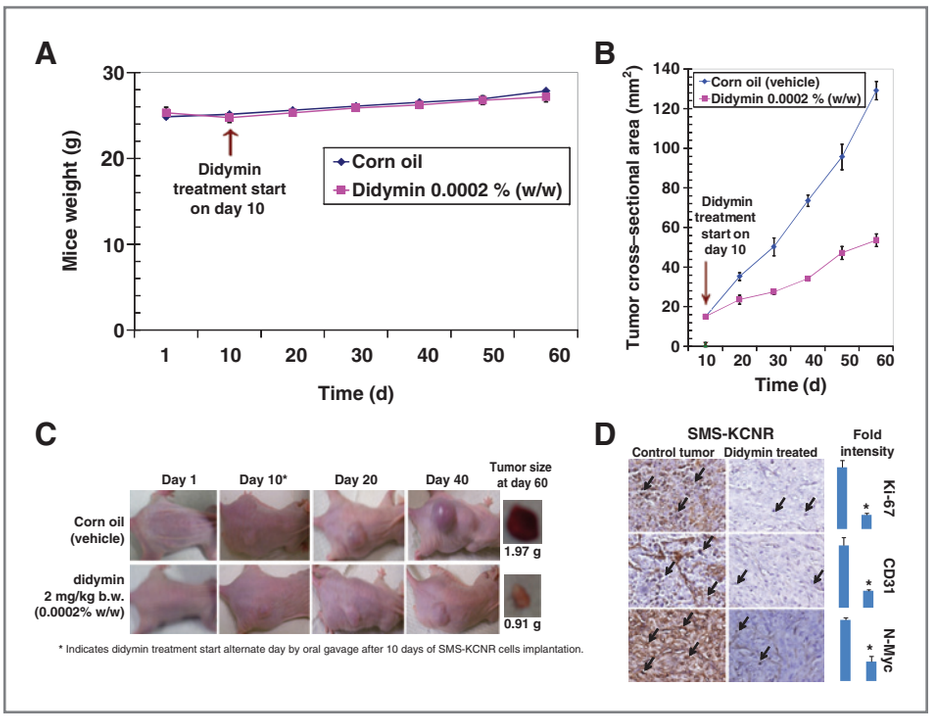

Figure 5. Effect of oral administration of didymin in *in vivo* mice xenograft study. Animals were examined daily for signs of tumor growth and body weights were recorded (A). Regression of SMS-KCNR neuroblastoma xenografts after didymin treatment in mice: Tumors were measured in 2 dimensions using calipers. Tumor cross-section revealing the regression of neuroblastoma tumors *in vivo* in didymin-treated group relative to controls (B). Photographs of animals and tumor were taken during the course of study (C). Impact of didymin treatment on the proliferation marker Ki67, angiogenesis marker CD31, and neuroblastoma oncogenic marker N-Myc expression in *in vivo* mice xenografts: Control- and didymin-treated SMS-KCNR neuroblastoma–bearing nude mice tumor sections were used for histopathologic analyses. IHC analyses for Ki67 expression (marker of cellular proliferation), CD31 (angiogenesis marker), and N-Myc (neuroblastoma oncogenic marker) from tumors in mice of control and didymin-treated groups were done. Statistical significance of difference was determined by 2-tailed Student *t* test. $P < 0.001$, didymin-treated compared with control. Immunoreactivity is evident as a dark brown stain, whereas nonreactive areas display only the background color. Arrows represent the area for positive staining for an antigen. The intensity of antigen staining was quantified by digital image analysis. Bars represent mean ± SE ($n = 5$); *, $P < 0.001$ compared with control (D).

transition, and decreased the migration of neuroblastoma cells *in vitro*. Importantly, didymin induced G_2/M cell-cycle arrest which was associated with decrease in the levels of cyclin B1, G_2/M phase regulator downstream of p53, and whose overexpression can override p53-induced G_2/M phase arrest (35). The downregulation of cyclin B1 explains one of the mechanisms responsible for the antiproliferative effect of didymin in both clinically sensitive p53-wild type and refractory p53 mutant neuroblastomas. Didymin did not cause any cytotoxicity in normal HUVEC cells as well as any overt toxicity in mice. Didymin strongly inhibited the proliferation (Ki67) and angiogenesis (CD31) markers as well as N-Myc expression *in vivo* mice xenograft studies.

Mechanistically, the inhibition of N-Myc by didymin, as elaborately confirmed at protein, mRNA, and promoter–reporter assays, was a hallmark of our studies. Amplification and overexpression of N-Myc is associated with both the incidence and refractoriness of neuroblastomas (5, 36). Hence, the ability of didymin to inhibit N-Myc at both transcriptional and translational levels reflects the significance of didymin toward developing novel interventional strategies for neuroblastomas. The nonbitter nature of didymin saves the time and effort spent on the investigations of taste-modifying additives for pediatric diets. As didymin is a highly palatable flavonoid, it can be possibly administered in milk or other liquid pediatric diets in the infants and adolescent children, who are usually not compatible with derivatized preparations such as pills and creams. Thus, didymin has both fundamental mechanistic and clinical as well as translational significance due to its potential to regulate critical nodes of neuroblastoma signaling which reflects its relevance to effectively prevent the incidence and progression of neuroblastomas (Fig. 6).

In summary, this study provides strong evidence for the "*N-Myc* inhibitory," "antiproliferative," and "antiangiogenic" properties of didymin with "no overt toxicity to normal cells and tissues" while characterizing potent anticancer effects *in vitro* cell cultures and *in vivo* mice xenograft models of neuroblastomas. This multispecific anticancer potential of didymin, which is of specific relevance to both the pathogenesis and progression of neuroblastomas, makes didymin a novel and highly relevant dietary agent for the treatment of neuroblastomas. Our studies also indicate that didymin is absorbed effectively following oral

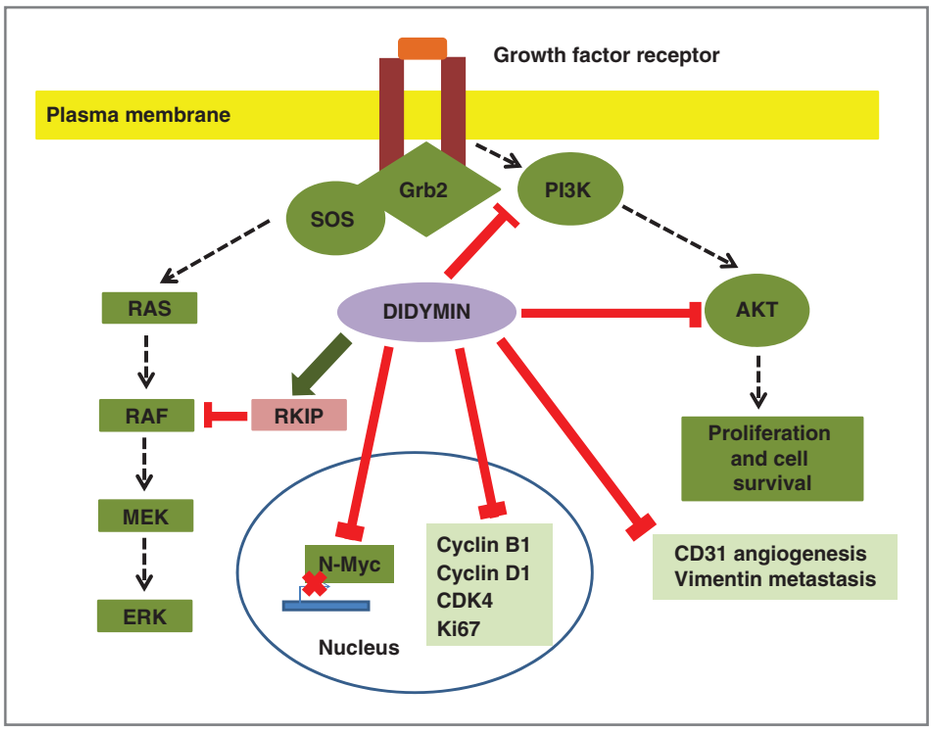

Figure 6. Effect of didymin signaling pathways in neuroblastoma. The novel flavonoid didymin inhibits N-Myc transcription. Didymin downregulated PI3K, Akt, vimentin, and upregulated RKIP. Didymin downregulated cyclin D1, CDK4, and, importantly, cyclin B1, which is downstream effector of p53-mediated cell-cycle regulation. Didymin decreased the angiogenic marker CD31, proliferation marker ki67 and N-Myc *in vivo* as revealed by histopathologic examination of resected tumors. Dotted arrows, normal signal transduction; normal arrows, upregulation of signaling protein due to didymin; T-shaped lines, inhibitory effect of didymin.

administration. In this context, the further studies focused on detailed absorption, distribution, metabolism, and excretion (ADME) kinetics of didymin should help to develop and test appropriate doses and formulations of didymin in milk and pediatric diets for use in children till 5 years, the high-risk window for the incidence of neuroblastomas. Collectively, didymin represents a novel and highly promising flavonoid with potential clinical significance to effectively prevent the incidence of neuroblastomas and also as an innovative approach for strategies proposed by **n**ew **a**pproaches for **n**euroblastoma **t**herapy (**NANT**) consortium.

Disclosure of Potential Conflicts of Interest

No potential conflicts of interest were disclosed.

Acknowledgments

The authors thank Dr. Sumihiro Suzuki, Department of Biostatistics, School of Public Health, UNTHSC, Fort Worth, TX, for his assistance in the statistical analyses of the data.

Grant Support

This work was supported in part by USPHS grant CA 77495, the Cancer Research Foundation of North Texas, and Institute for Cancer Research & the Joe & Jessie Crump Fund for Medical Education.

The costs of publication of this article were defrayed in part by the payment of page charges. This article must therefore be hereby marked *advertisement* in accordance with 18 U.S.C. Section 1734 solely to indicate this fact.

Received June 21, 2011; revised November 11, 2011; accepted December 10, 2011; published OnlineFirst December 15, 2011.

References

1. Smith SJ, Diehl N, Leavitt JA, Mohney BG. Incidence of pediatric Horner syndrome and the risk of neuroblastoma: a population-based study. Arch Ophthalmol 2010;128:324–9.
2. Jacob ES, Varghese RG, Toi PC, Bhaskaran R, Rai R. Congenital neuroblastoma with liver metastasis presenting with Hashimoto Pritzker disease. Ind J Pathol Microbiol 2009;52:374–6.
3. DuBois SG, Kalika Y, Lukens JN, Brodeur GM, Seeger RC, Atkinson JB, et al. Metastatic sites in stage IV and IVS neuroblastoma correlate with age, tumor biology, and survival. J Pediatr Hematol Oncol 1999;21:181–9.
4. Janardhanan R, Banik NL, Ray SK. N-Myc down regulation induced differentiation, early cell cycle exit, and apoptosis in human malignant neuroblastoma cells having wild type or mutant p53. Biochem Pharmacol 2009;78:1105–14.
5. Weiss WA, Aldape K, Mohapatra G, Feuerstein BG, Bishop JM. Targeted expression of MYCN causes neuroblastoma in transgenic mice. EMBO J 1997;16:2985–95.
6. Keshelava N, Zuo JJ, Chen P, Waidyaratne SN, Luna MC, Gomer CJ, et al. Loss of p53 function confers high-level multidrug resistance in neuroblastoma cell lines. Cancer Res 2001;61:6185–93.
7. Trakul N, Rosner MR. Modulation of the MAP kinase signaling cascade by raf kinase inhibitory protein. Cell Res 2005;15:19–23.
8. Fu Z, Smith PC, Zhang L, Rubin MA, Dunn RL, Yao Z, et al. Effects of Raf kinase inhibitor protein expression on suppression of prostate cancer metastasis. J Natl Cancer Inst 2003;95:878–89.
9. Yeung K, Janosch P, McFerran B, Rose DW, Mischak H, Sedivy JM, et al. Mechanism of suppression of the Raf/MEK/extracellular signal-regulated kinase pathway by the Raf kinase inhibitor protein. Mol Cell Biol 2000;20:3079–85.
10. Singhal J, Yadav S, Nagaprashantha L, Vatsyayan R, Singhal SS, Awasthi S. Targeting p53 null neuroblastomas through RLIP76. Cancer Prev Res 2011;4:879–89.

11. Singhal SS, Wickramarachchi D, Yadav S, Singhal J, Leake K, Vatsyayan R, et al. Glutathione-conjugate transport by RLIP76 is required for clathrin-dependent endocytosis and chemical carcinogenesis. Mol Cancer Ther 2011;10:16–28.
12. Hung JY, Hsu YL, Ko YC, Tsai YM, Yang CJ, Huang MS, et al. Didymin, a dietary flavonoid glycoside from citrus fruits, induces Fas-mediated apoptotic pathway in human non-small-cell lung cancer cells *in vitro* and *in vivo*. Lung Cancer 2010;68:366–74.
13. Marimpietri D, Brignole C, Nico B, Pastorino F, Pezzolo A, Piccardi F, et al. Combined therapeutic effects of vinblastine and rapamycin on human neuroblastoma growth, apoptosis, and angiogenesis. Clin Cancer Res 2007;13:3977–88.
14. Modak S, Cheung NK. Neuroblastoma: Therapeutic strategies for a clinical enigma. Cancer Treat Rev 2010;36:307–17.
15. Singhal SS, Sehrawat A, Sahu M, Singhal P, Vatsyayan R, Lelsani P, et al. Rlip76 transports sunitinib and sorafenib and mediates drug resistance in kidney cancer. Int J Cancer 2010;126:1327–38.
16. Singhal SS, Singhal J, Yadav S, Sahu M, Awasthi YC, Awasthi S. RLIP76: A target for kidney cancer therapy. Cancer Res 2009;69: 4244–51.
17. Singhal SS, Yadav S, Drake K, Singhal J, Awasthi S. Hsf-1 and POB1 induce drug sensitivity and apoptosis by inhibiting Ralbp1. J Biol Chem 2008;283:19714–29.
18. Singhal SS, Yadav S, Singhal J, Zajac E, Awasthi YC, Awasthi S. Depletion of RLIP76 sensitizes lung cancer cells to doxorubicin. Biochem Pharmacol 2005;70:481–8.
19. Lee HC, Tian B, Sedivy JM, Wands JR, Kim M. Loss of raf kinase inhibitor protein promotes cell proliferation and migration of human hepatoma cells. Gastroenterology 2006;131:1208–17.
20. Santos SD, Verveer PJ, Bastiaens PI. Growth factor-induced MAPK network topology shapes erk response determining PC-12 cell fate. Nat Cell Biol 2007;9:324–30.
21. Singhal J, Singhal SS, Yadav S, Suzuki S, Warnke MM, Yacoub A, et al. RLIP76 in defense of radiation poisoning. Int J Radiat Oncol Biol Phys 2008;72:553–61.
22. Baskin DS, Ngo H, Didenko VV. Thimerosal induces DNA breaks, caspase-3 activation, membrane damage, and cell death in cultured human neurons and fibroblasts. Toxicol Sci 2003;74:361–8.
23. Rosenberg Zand RS, Jenkins DJ, Brown TJ, Diamandis EP. Flavonoids can block PSA production by breast and prostate cancer cell lines. Clin Chim Acta 2002;317:17–26.
24. Lillington DM, Goff LK, Kingston JE, Onadim Z, Price E, Domizio P, et al. High level amplification of N-Myc is not associated with adverse histology or outcome in primary retinoblastoma tumors. Br J Cancer 2002;87:779–82.
25. Ito Y, Otsuki Y. Localization of apoptotic cells in the human epidermis by an in situ DNA nick end-labeling method using confocal reflectant laser microscopy. J Histochem Cytochem 1998;46:783–6.
26. Tseng YH, Chang KW, Yang CC, Liu CJ, Kao SY, Liu TY, et al. Association between areca-stimulated vimentin expression and the progression of head and neck cancers. Head Neck 2011; Mar 7 [Epub ahead of print].
27. McInroy L, Maatta A. Down-regulation of vimentin expression inhibits carcinoma cell migration and adhesion. Biochem Biophys Res Commun 2007;360:109–14.
28. Hede SM, Nazarenko I, Nister M, Lindstrom MS. Novel perspectives on p53 function in neural stem cells and brain tumors. J Oncol 2011;2011:852970.
29. Paolella BR, Havrda MC, Mantani A, Wray CM, Zhang Z, Israel MA. p53 directly represses Id2 to inhibit the proliferation of neural progenitor cells. Stem Cells 2011;29:1090–101.
30. Taylor WR, Stark GR. Regulation of the G2/M transition by p53. Oncogene 2001;20:1803–15.
31. Stacey DW. Cyclin D1 serves as a cell cycle regulatory switch in actively proliferating cells. Curr Opin Cell Biol 2003;15: 158–63.
32. Guo Y, Stacey DW, Hitomi M. Post-transcriptional regulation of cyclin D1 expression during G2 phase. Oncogene 2002;21: 7545–56.
33. Gabrielli BG, Sarcevic B, Sinnamon J, Walker G, Castellano M, Wang XQ, et al. A cyclin D-Cdk4 activity required for G2 phase cell cycle progression is inhibited in ultraviolet radiation-induced G2 phase delay. J Biol Chem 1999;274:13961–9.
34. Yin F, Giuliano AE, Law RE, Van Herle AJ. Apigenin inhibits growth and induces G2/M arrest by modulating cyclin-CDK regulators and ERK MAP kinase activation in breast carcinoma cells. Anticancer Res 2001;21:413–20.
35. Woo KJ, Lee TJ, Bae JH, Jang BC, Song DK, Cho JW, et al. Thimerosal induces apoptosis and G2/M phase arrest in human leukemia cells. Mol Carcinog 2006;45:657–66.
36. Chen Q, Zhang X, Jiang Q, Clarke PR, Zhang C. Cyclin B1 is localized to unattached kinetochores and contributes to efficient microtubule attachment and proper chromosome alignment during mitosis. Cell Res 2008;18:268–80.
37. Innocente SA, Abrahamson JL, Cogswell JP, Lee JM. p53 regulates a G2 checkpoint through cyclin B1. Proc Natl Acad Sci U S A 1999;96:2147–52.
38. Park M, Chae HD, Yun J, Jung M, Kim YS, Kim SH, et al. Constitutive activation of cyclin B1-associated cdc2 kinase overrides p53-mediated G2-M arrest. Cancer Res 2000;60:542–5.
39. Kang J, Rychahou PG, Ishola TA, Mourot JM, Evers BM, Chung DH. N-myc is a novel regulator of PI3K-mediated VEGF expression in neuroblastomas. Oncogene 2008;27:3999–4007.
40. Chesler L, Schlieve C, Goldenberg DD, Kenney A, Kim G, McMillan A, et al. Inhibition of phosphatidylinositol 3-kinase destabilizes Mycn protein and blocks malignant progression in neuroblastoma. Cancer Res 2006;66:8139–46.
41. Chatterjee D, Bai Y, Wang Z, Beach S, Mott S, Roy R, et al. RKIP sensitizes prostate and breast cancer cells to drug-induced apoptosis. J Biol Chem 2004;279:17515–23.
42. Dangi-Garimella S, Yun J, Eves EM, Newman M, Erkeland SJ, Hammond SM, et al. Raf kinase inhibitory protein suppresses a metastasis signalling cascade involving LIN28 and let-7. EMBO J 2009;28: 347–58.
43. Yeung K, Seitz T, Li S, Janosch P, McFerran B, Kaiser C, et al. Suppression of Raf-1 kinase activity and MAP kinase signalling by RKIP. Nature 1999;401:173–7.
44. Hellmann J, Rommelspacher H, Muhlbauer E, Wernicke C. Raf kinase inhibitor protein enhances neuronal differentiation in human SH-SY5Y cells. Dev Neurosci 2010;32:33–46.